Journal of Analysis and Testing
https://doi.org/10.1007/s41664-024-00333-y

REVIEW

Recent Progress in the Construction of Chiral Plasmonic Gold Nanostructures and Their Biochemical Sensing Applications

Liangtong Li[1,2] · Fu Zhu[1,2] · Yuxuan Tang[1,2] · Donghai Zhu[1] · Lijuan Wang[1] · Jian Wang[2]

Received: 15 February 2024 / Accepted: 13 July 2024

Abstract
Chirality, as the asymmetric property of nature, cannot fit its mirror image by translation or rotation. It is widespread from small molecules to the vast universe, including the asymmetric nanomaterials. Especially, chiral nanomaterials exhibit unique optical and optomechanical effects, as well as the outstanding biological stereoselectivity, which have attracted great attention. With the great progress made in chemical synthesis of nanomaterials, chiral plasmonic gold nanomaterials with various sizes and morphologies have become increasingly accessible, putting forward the research and development of chirality. Recently, the chiral molecular linkers, chiral templates, or chiral assembly of plasmonic nanomaterials have been rapidly developed, promoting the great promise of plasmonic circular dichroism (PCD) from metal nanomaterials in enantioselective catalysis, chiral separation, and sensitive detection. This work reviews various types of chiral nanostructures and their synthetic strategies of typical chiral gold nanomaterials, and further introduces their biochemical sensing application.

Keywords Chirality · Circular dichroism · Gold nanostructures · g-factor · Biosensing

1 Introduction

One of the most fascinating properties of nature is chirality [1–3], which plays an important role in the origin of life. Just like DNA/RNA is composed of residues with the same chirality, life on earth also exhibits the priority of L-amino acids and D-sugars [4]. Moreover, many natural objects, such as human hands, gourd tendrils, snail shells, and even helix nebulae, exhibit chirality [5]. In addition, the biological activity of many chiral molecules also depends on their chirality. For example, one of the molecule enantiomer can be used as medicine because of its high biological activity, but the other one is toxic [6]. In short, chirality plays a crucial role in the structural properties of themselves and their interactions with external substances. Therefore, the investigation of chirality is of great significance in various fields, such as biology, physical chemistry, medicine, and modern technology, including stereoscopic displays, data storage devices, photon routers [7, 8].

Plasmonic nanomaterials present good and stable physicochemical, optical, electrochemical, and biological properties, which have attracted great attention for a long time [9]. Among them, gold nanoparticles (AuNPs) have been widely studied because of their low toxicity and excellent performance in various applications such as catalysis, energy storage, separation, adsorption, and chemical sensing [10–18]. Especially, the intrinsic localized surface plasmon resonance (LSPR) feature [19, 20] significantly enhances the photo-matter interaction at the nanoscale. When chirality is introduced to AuNPs, they exhibit strong chiral optical properties due to their LSPR, which endows them with plasmonic circular dichroism (PCD) [21] over a wide range from visible to near-infrared region [22]. Usually, the chiral plasmonic AuNPs could be effectively used to investigate the chirality origin and applications of nanoparticles (NPs) [1]. So developing more different chiral AuNPs will offer favorable opportunities for chiral applications, such as biosensing based on plasmonic chiral response [23–27], biological imaging [27, 28], isomer

✉ Lijuan Wang
wlj.wang@163.com

✉ Jian Wang
wj123456@swu.edu.cn

[1] Basic Medical Teaching Department, Shangqiu Medical College, Shangqiu 476299, China

[2] Key Laboratory of Biomedical Analytics (Southwest University), Chongqing Science and Technology Bureau, College of Pharmaceutical Sciences, Southwest University, Chongqing 400715, China

Published online: 18 September 2024

separation and recognition [29], and disease diagnosis [30–32].

The circular dichroism (CD) effect is related to the molecular absorption of clockwise and counterclockwise circularly polarized light and CD spectra, which is a potential signal for revealing molecular chirality and conformational analysis in chemical reactions [33]. The chiral optical response of plasmonic NPs can be adjusted and enhanced by the integration of LSPR properties [34], including (I) intrinsic chirality depending on the geometric shape of NPs [35], (II) structural chirality of chiral nanoassemblies induced by chiral templates or linkers [36], and (III) coupled chirality between chiral molecules and non-chiral plasmonic NPs [37]. Due to the interaction between weak molecular dipoles and plasmon dipoles, simple chiral molecular attachment methods typically cannot obtain high PCD [1]. By taking advantage of wet chemical synthesis or chiral self-assembly process, nanomaterials with high discrete CD, which correspond to these two types of synthesis methods, namely, discrete chiral plasmonic nanostructures and chiral plasmonic superstructure, can be obtained. [38]. This review briefly describes the synthesis strategies of different types of chiral gold nanostructures (Scheme 1), as well as their biosensing applications in recent years.

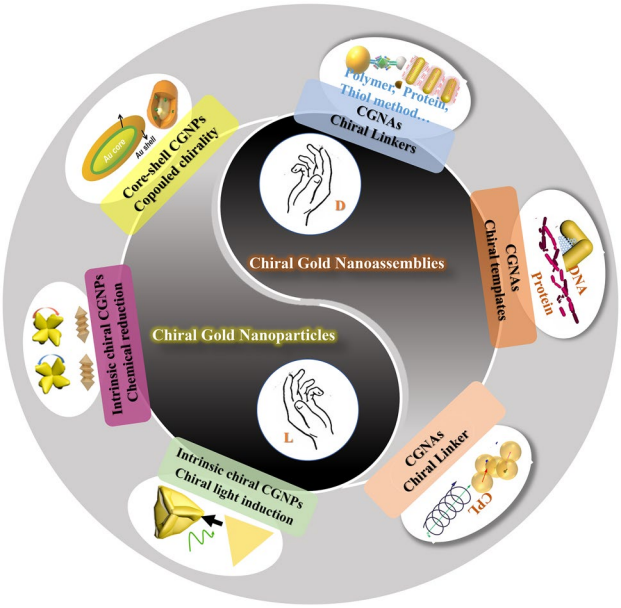

Scheme 1 The construction of chiral gold nanostructures

2 Single Chiral Gold Nanoparticles

The synthetic approaches of nanostructures mainly include hard film plate method based on photolithography technology and the wet chemical synthesis method in solution [9]. The single chiral gold nanoparticles (CGNPs) synthesized by the top-down method have limited applications due to their poor crystal, single category, and high cost, which are rarely used compared with other superior methods [39]. What's more, biological green synthesis of CGNPs has not yet been deeply conducted, and their homogeneity and production capacity are also limited [40]. Therefore, nowadays, CGNPs are mainly obtained through wet chemical synthesis.

Wet chemical synthesis includes chemical reduction, electrochemical, and photochemical methods [7]. Among these, the seed growth method in the chemical reduction method and the photo-induced method in the photochemical method are the most used in the synthesis of CGNPs. The seed growth method employs ligand-mediated seed regrowth to precisely and conveniently modulate the morphology and size of NPs [41]. There are usually two representative pathways for obtaining CGNPs based on seed-mediated growth. One is to utilize non-chiral NPs as seeds, embedding chiral ligands at the hotspots of the interface or cavity through shell growth or obtaining an irregular shell to adsorb chiral molecules at the tip or gap hotspots. The obtained core–shell nanostructures exhibit significant chiral optical activity, resulting from the hotspot enhanced chiral interactions, but they may not necessarily present the chiral morphology. The other also uses non-chiral NPs as seeds, the difference is that the regrowth mediated by chiral molecules can lead to the formation of chiral three-dimensional (3D) morphology. The inherent chirality of the chiral morphology of nanomaterials is the main source of PCD signals. Regarding photo-induced chemical synthesis, the chiral polarized light is used to induce chiral growth of seeds, thus enabling the production of NPs with enhanced chiral signals. However, chiral ligands are not a prerequisite in this synthesis process [42].

2.1 Chiral Molecules-Coupled Gold Nanoparticles

Due to the weak interaction between molecular dipoles and plasmons, simple adsorption or encapsulation of chiral molecules on NPs surfaces can only induce a weak CD response. However, the strong optical coupling between plasmon and chiral molecules can be employed to obtain enhanced chiral AuNPs. Liu et al. obtained gold nanorod@chiral mesoporous silica core–shell NPs (GNR@CMS NPs) by growing a mesoporous silica shell filled with chiral molecules on the surface of gold nanorods (AuNRs) [43] (Fig. 1a). Its unique plasmon-induced CD signal stems from the powerful optical coupling between the embedded chiral molecules and core–shell NPs. Further research has demonstrated that modifying the aspect ratio of AuNRs can effectively regulate the chirality of core–shell NPs across a broad spectrum. The CD signal and surface-enhanced Raman

scattering (SERS) of these materials could be employed for the identification of chiral enantiomers. In addition, for single NPs, plasmonic field enhancement can also significantly improve PCD response by trapping chiral molecules in hotspots, because of plasmon coupling enhancing localized field [44]. However, the reasonable design of such hotspots still needs to be explored.

Usually, most gold core–shell structures do not present the obvious chiral morphology. For example, Zheng et al. constructed chiral AuNRs (c-AuNRs) with the mediation of L-cysteine (Cys) and D-Cys (Fig. 1b) using a program similar to a carambola-shaped AuNRs [45]. By adjusting the concentration of Cys, c-AuNRs with different morphologies were obtained. Among them, c-AuNRs with one or two spikes were obtained at a lower concentration of Cys (4 nM), exhibiting a significant PCD response, which is due to the appropriate embedding of Cys in the hotspot cavities inside the interfaces of core–shell. The change in morphology mostly originates from the adsorbed chiral thiols on the surface, but it is not the major chiral source of this type of CGNPs. Yan et al. used chiral mercaptans (Cys) as modulation molecules to obtain high PCD response carambola-shaped AuNPs with anisotropic g-factor about -0.005 by overgrowth of AuNRs [46] (Fig. 1c). It was found that the PCD signal mainly comes from the contribution of the formation of hotspots of chiral Cys molecules in the shell cavities, but the pre-adsorbed Cys molecules did not contribute to the PCD signal, and their role was mainly to manipulate the growth mode of Au. In addition, the free Cys molecules were the chiral contributor, resulting from the remaining Cys molecules on the shell to form a hotspot. This work took advantage of chiral molecules with thiol groups to modulate the interface of AuNRs surface, providing a unique method for preparing AuNPs with high chiral activity through a simple regrowth procedure.

Mediating the adsorption or growth of chiral molecules within particle structures with surfactants is a straightforward process that can yield robust chiral signals [47]. The underlying mechanism of chiral enhancement is attributed to the formation of hotspots by the dipole–dipole interaction between chiral molecules and plasmonic AuNPs. A number of CGNPs employing hotspots have been developed, such as the chiral hotspots of gaps between two or more non-chiral AuNPs by Lin et al. [48] and Hiromasa et al. [49], the chiral hotspots within nanopores on gold substrates by Wang et al. [50], and the chiral application of hotspots between surface folds of intrinsic chiral nanoparticles by Wu's group [51].

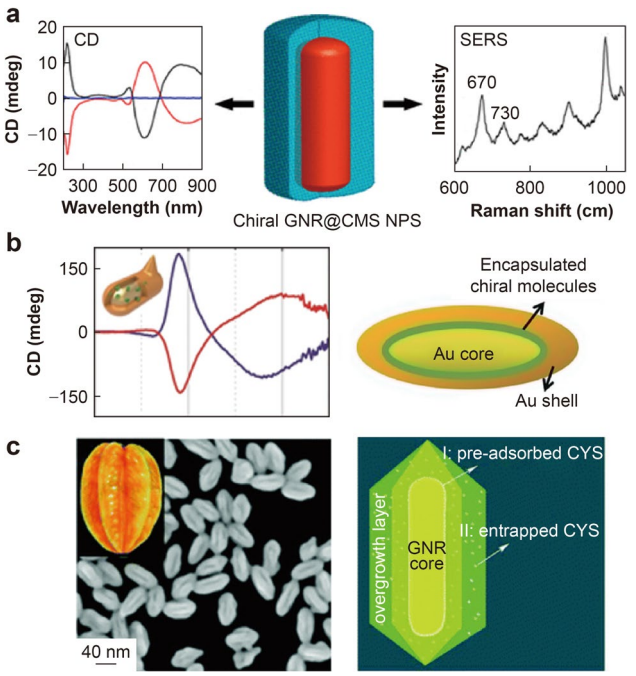

Fig. 1 Schematic illustration of single CGNPs with coupled chirality. **a** The structures and signals of GNR@CMS NPs (Reprinted with permission from Ref. [43]. Copyright © 2013 American Chemical Society). **b** The core–shell structures of c-AuNRs (Reprinted with permission from Ref. [45]. Copyright © 2018 WILEY–VCH Verlag GmbH & Co. KGaA, Weinheim). **c** The core–shell structures of star-fruit-like chiral AuNRs (Reprinted with permission from Ref. [46]. Copyright © 2017 Royal Society of Chemistry)

2.2 Intrinsic Chiral Gold Nanoparticles

2.2.1 Seed-Mediated Regrowth Method

With the development of wet chemistry synthesis, it is more convenient to accurately construct AuNPs with different morphologies and sizes. However, these chiral NPs do not possess chiral 3D structures, and their chirality are mainly caused by the hotspot effects of chiral molecules rather than inherent chirality caused by chiral shapes. The leap in the synthesis of 3D CGNPs dominated by inherent chirality occurred when Nam et al. [52] synthesized a 3D gold spiral cube with a strong PCD response. This method pioneered the strong chiral ligands to mediate the synthesis of chiral AuNPs with chiral morphology. This was a one hundred nanometer scale chiral AuNPs with adjustable chiral plasmonic resonance (Fig. 2a), which was obtained by using non-handed cubic or octahedron AuNPs as gold seed and guided by chiral peptides or Cys molecules.

The enantioselective interaction between chiral ligands and the surface of nano-seeds gives rise to variations in the regrowth rate of chiral facets, which in turn results in forming helical wrinkles in the NPs. Moreover, the maximum g-factor of chiral NPs approximately 0.2 can be obtained under the optimized growth conditions. In addition, when the strategy was extended to palladium (Pd) NPs as seeds, the obtained Pd NPs did not exhibit significant PCD reactions. It is supposed that it was due to the weak interaction between thiols and the Pd surface, as well as the low chiral

specification of chiral thiols on the high refractive index on the Pd surface.

Following the pioneering research conducted by Nam's team, a significant number of 3D CGNPs have been reported. For example, Chen et al. developed a non-chiral thiol assisted growth strategy to synthesize discrete chiral helical plasmonic nanorods (HPNR) with strong and tunable PCD response [53]. After mixing AuNRs with Cys and 4-aminoneneneba thiophenol (4-ATP), Au was used as a seed to support the following growth of spiral Au and Ag alloy shells. By optimizing the growth parameters, a high PCD response with a g-factor value of approximately 0.04 was obtained. Herein, Cys was regarded as an indispensable role in the development of helical shells, whereas achiral thiol 4-ATP serves a supplementary function in rectifying imperfections of structure, thereby improving the plasmonic chiral signals. Chen et al. [54] and Gao et al. [55] have additionally elucidated the helical morphology and the mechanism of chirality formation in HPNRs (Fig. 2b). The finite difference time domain (FDTD) simulation verifies that the plasmonic chirality response came from the helical morphology, which was consistent with the experimental results. Therefore, the combination of chiral Cys and non-chiral 4-ATP enriches the synthesis of CGNPs.

Meanwhile, some researchers also have obtained HPNR by using AuNRs as the seed for chiral induction under selenocysteine and ultraviolet irradiation [24]. Zhang et al. used gold nanooctopuses (AuNOPs) as seeds and obtained chiral AuNOPs through eight overgrowth steps in the presence of glutathione (GSH) [56], which depicted a propeller structure (Fig. 2c) exhibiting configuration with eight arms oriented from <111> to <100> directions. Ni et al. [57] described an optimized chiral growth method for preparing fourfold twisted AuNRs (Fig. 2d). $HAuCl_4$ as a chiral inducer after being reduced with cysteine, and ascorbic acid as a reducing agent, four inclined ridges and a strong chirality with

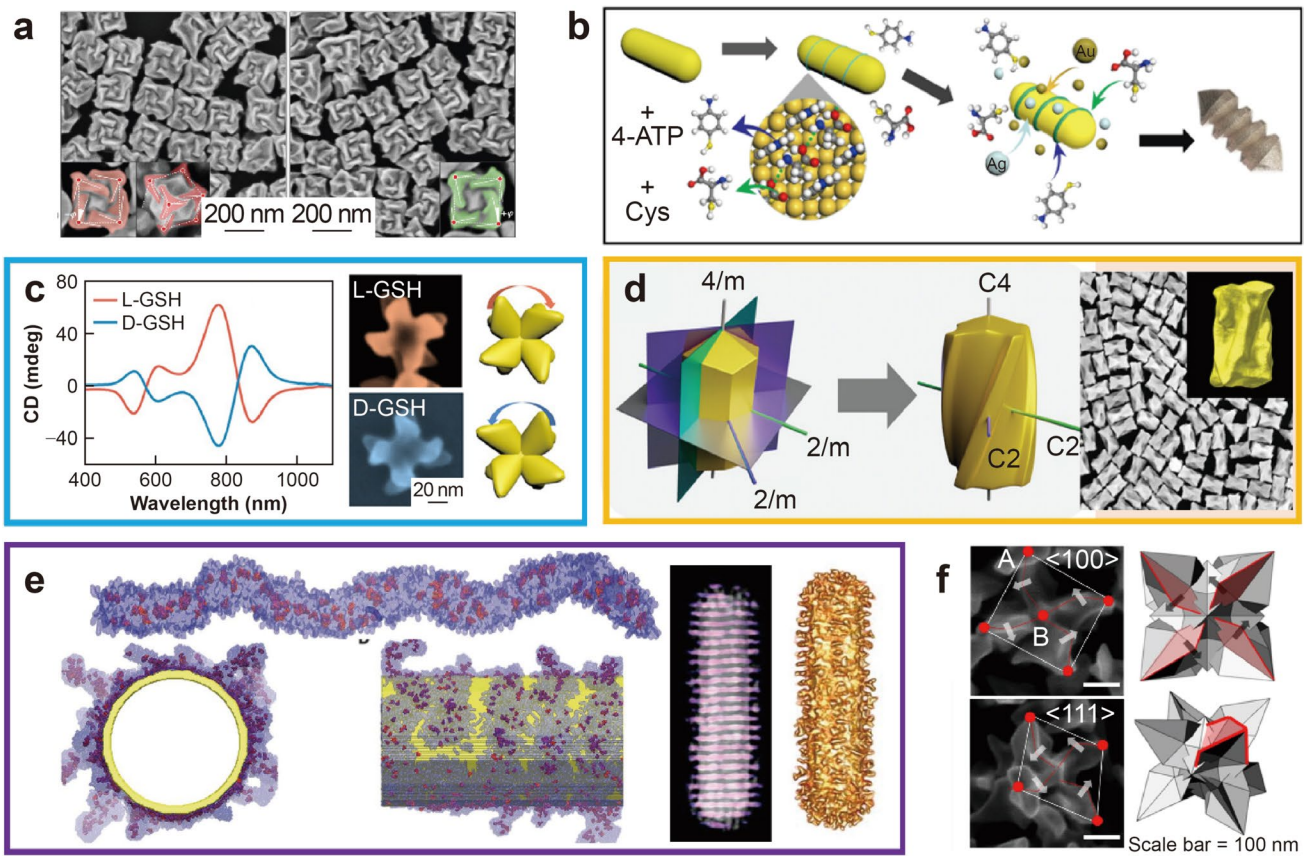

Fig. 2 Schematic illustration of chiral gold nanostructures with different morphologies. **a** The SEM image of gold helix chiral nanocubes (Reprinted with permission from Ref. [52] Copyright © 2018 Springer Nature Ltd.). **b** The synthesis of HPNRs (Reprinted with permission from Ref. [54]. Copyright © 2023 Springer-Verlag Berlin Heidelberg). **c** The shape of chiral AuNOPs (Reprinted with permission from Ref. [56] Copyright © 2022 Chinese Chemical Society). **d** The structure of fourfold twisted chiral AuNRs (Reprinted with permission from Ref. [57] Copyright © 2023 WILEY–VCH Verlag GmbH & Co. KGaA, Weinheim). **e** The morphology of chiral AuNPs induced by wormlike chiral micelles (Reprinted with permission from Ref. [60] Copyright © 2020 American Association for the Advancement of Science). **f** The morphology of chiral AuNPs directionally synthesized from adenine oligomers (Reprinted with permission from Ref. [61] Copyright © 2022 Springer Nature Ltd.)

a maximum g-factor (g_{max}) of −0.106 were found on the surface of the single crystal-nanorods, suggesting that the asymmetry was due to the appearance of chiral surfaces in the form of protrusions on the initial nanorods, ultimately leading to the distorted shapes.

There are many chiral AuNPs synthesized with strong chiral ligands as mediators. For example, chiral gold nanoarrowheads (AuNAs) by using L-$SeCys_2$ as a chiral inducer, and AuNRs as a seed [24]; chiral trihedral AuNPs by controlling overgrowth process with binary surfactant [25]; propeller shaped chiral gold nanotriangles [23], as well as the chiral helical gold nanocubes induced by chiral Cys/GSH or dipeptides [58, 59].

Taking the advantages of seed growth method of obtaining chiral 3D AuNPs strategies, the diverse varieties of chiral NPs have been developed. As the most used synthesis method at present, seed growth method is easy to operate, which endows chiral NPs with strong chirality, high stability, and adjustable 3D morphology [2]. In addition to the strong chiral ligands, weak chiral ligands can also mediate the synthesis of AuNPs with chiral morphology. Rubio et al. [60] used weak chiral ligands including 2-naphthol and R-/S-1.1′-binaphthyl-2.2′-diamine to induce wormlike chiral micelles (Fig. 2e). By introducing them into the growth solution containing cetyltrimethylammonium chloride (CTAC) micelles, the chiral AuNPs with g-factor about 0.2 were obtained by chiral mercaptan mediated growth. They speculated that the adsorption of chiral micelles on the surface of AuNRs formed chiral and worm like aggregates and the chiral structure of aggregates was transferred to the deposited metal shell during the growth process.

Chiral cosurfactant induced growth clearly provides another useful pathway for the synthesis of discrete chiral NPs. In addition, single stranded DNA (ssDNA) can be used as chiral shape modifiers to synthesize chiral AuNPs [61]. The results showed that the isotype ssDNA composed of adenine nucleobase could make the gold nanooctahedron seeds grow into chiral gold nanostars with eight curved sides with obvious 3D chiral structure (Fig. 2f), and its asymmetry g-factor was as high as 0.04 at visible light wavelength.

2.2.2 Photochemical Synthesis Method

As well known, photochemical methods can be used for the synthesis of various AuNPs. Similar to the initial electrochemical method used, it does not require the addition of any reducing agent in the growth solution. Energy is provided for the reaction through ultraviolet irradiation, and noble metal nanorods with different aspect ratios are synthesized by changing the concentrations. Besides the preparation of AuNRs, photochemical methods can also be used to drive the shell deposition of AuNRs. Recently, Xu et al. [62] introduced circularly polarized light (CPL) into the construction of CGNPs, thereby further enhancing the chiral optical activity of chemically synthesized discrete chiral plasmonic NPs to a new degree (g_{max} of approximately 0.44) (Fig. 3a). The synthesis of chiral gold nanocubes was grown by employing Au nanoprisms as seeds and a chiral cysteine-phenylalanine (CYP) dipeptide as a medium under light irradiation with a wavelength overlapping with the localized surface plasmon resonance of the seeds. Its chirality is significantly higher than that of chiral gold nanocubes obtained by ordinary seed growth methods [52]. It is also found that the photochemical growth of chiral NPs is coupled with the chiral transfer of photons to the NPs. Specifically, when left CPL is used to assist left dipeptides, the strongest CD signal can be observed. And the sides with propeller like concave convex structures on the surface of different chirality also exhibit different rotation directions. Interestingly, the helical direction of folds in CGNPs with different chirality is determined by the chirality of the ligand, but the curvature and depth of the folds are controlled by the illumination.

In addition, some chiral AuNPs, such as the HPNR synthesized by Wen et al. [24] using chiral selenocysteine, also require UV light induction, otherwise only chiral gold nanoarrows can be obtained. It is evident that these photo-induced methods, similar to the seed growth method of chemical reduction, are inseparable from the chiral ligands. Of course, chiral ligands are not a prerequisite; but CPL as the sole chiral source, can also result in the formation of discrete intrinsic CGNPs. Koichiro et al. [63] employed site-selective oxidation–reduction induced by CPL to deposit platinum oxide on different edges of non-chiral gold nanocuboids, ultimately resulting in chiral gold nanocuboids with different chirality. Kazeto et al. [64] further introduced ultraviolet light to redox PtO_2, allowing for reversible chiral switching of gold nanomaterials with changes in CPL (Fig. 3b). This switchable strong CGNPs has great application prospects in chiral sensors and data storage.

The pure CPL induction is also limited in conveniently obtaining high-quality CGNPs, which requires a clear mechanism explanation. Lee et al. [42] conducted a detailed investigation on the synthesis mechanism of chiral AuNCs induced by CPL (Fig. 3c). They used single particle analysis techniques combined with theoretical simulation of the electronic surface mapping of NPs, and found that the asymmetric distribution of hot electrons on non-chiral AuNCs under CPL excitation mediated the plasmon-induced chiral transfer. Furthermore, the chiral transfer has been investigated for its potential applications in chiral growth in bimetallic systems. Additionally, the theoretical research and applications exploration of chiral light-matter interaction are of great significance for the design and optimization of future chiral sensors and chiral catalysis.

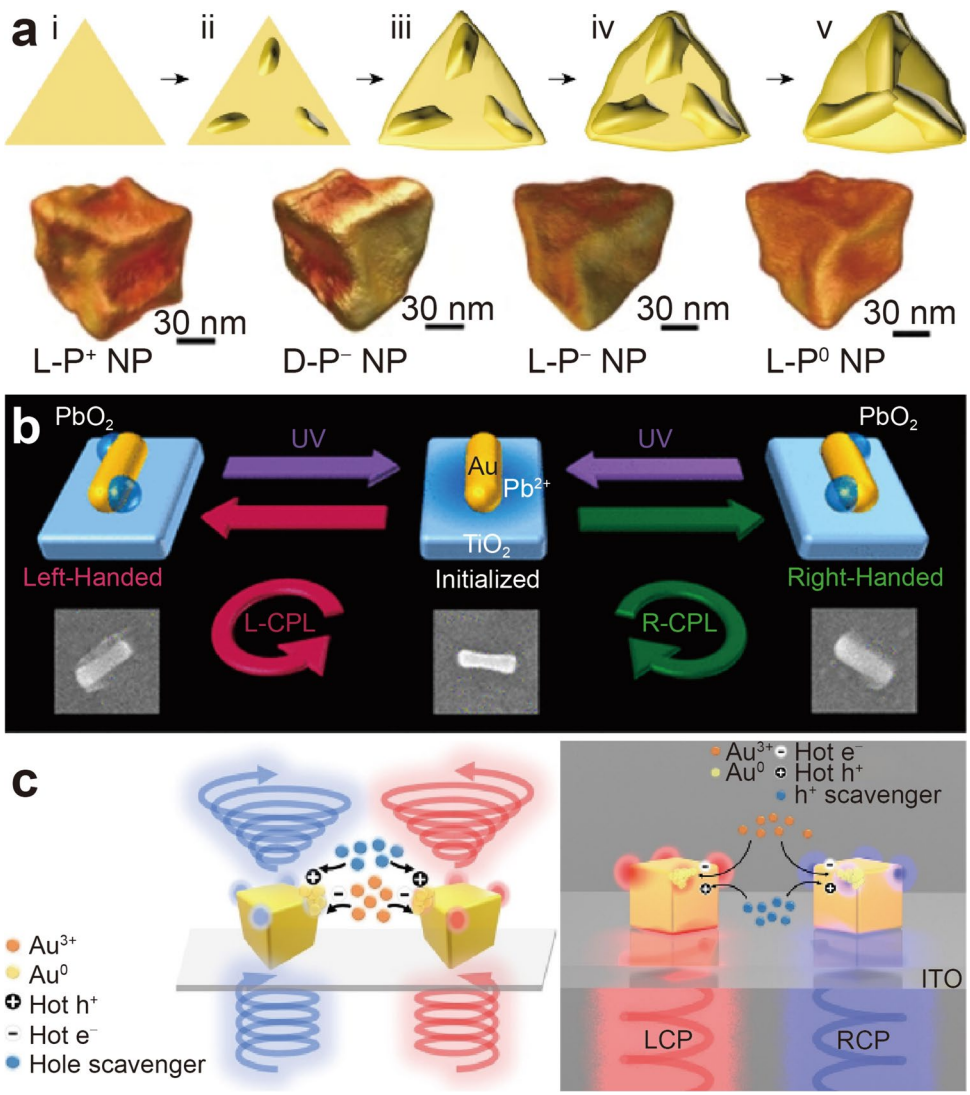

Fig. 3 Schematic illustration of CGNPs induced by photochemical method. **a** Simulation diagram of the growth process and morphology of chiral gold nanocubes synthesized by photo-induction (L/D represents left and right circularly polarized light irradiation, and ± represents dipeptide chirality). (Reprinted with permission from Ref. [62] Copyright © 2022 Springer Nature Limited). **b** Schematic diagram of chiral switching of photo-induced chiral gold nanorods (Reprinted with permission from Ref. [64] Copyright © 2020 American Chemical Society). **c** Schematic diagram of the mechanism of pure CPL induced intrinsic chiral AuNCs (Reprinted with permission from Ref. [42] Copyright © 2024 WILEY–VCH Verlag GmbH & Co. KGaA, Weinheim)

3 Chiral Gold Nanoassemblies

The construction of chiral gold nanoassemblies (CGNAs) is primarily achieved through a bottom-up assembly of AuNPs guided by various chiral molecules or templates. The main methods include (1) synthesis with chiral small molecules, biomacromolecules (DNA, peptide/protein), or chiral polymers as chiral connectors or as chiral driving molecules when adsorbed on the NPs' surface; (2) guiding the chiral assemblies of AuNPs with chiral templates, such as fibers, hydrogels, protein aggregates, and DNA origami. Especially, the advancement of DNA origami technology has facilitated the precise regulation of the spatial configuration of internal NPs in CGNAs, promoting the creation of chiral plasmonic superstructures with a robust chiral optical response [7]; and (3) other methods, such as assembling AuNPs into chiral superstructures without introducing additional chiral substances under the drive of circularly polarized light [65].

3.1 Chiral Molecular Linkers

Using chiral molecules as chiral junctions or chiral drivers for chiral gold superstructures is an effective approach to obtain the CGNAs. On one hand, chiral molecules can act as ligands to exert chirality on the obtained nanocomponents; on the other hand, they can serve as drivers or linkers to assemble AuNPs into chiral structures. As mentioned above, small biomolecules, including amino acids and thiol compounds, are more easily and controllably coupled to the surface of AuNPs due to their simple structure and small steric hindrance effects. In addition, the direction and accessibility of small molecules can be precisely controlled without reducing biological activity. Therefore, AuNPs functionalized with small biomolecules can become more stable and reproducible during biochemical analysis [66]. Meng et al. [67] developed a novel method for forming CGNAs by assembling discrete AuNRs with chiral thiols. Following

the adsorption of mercaptan, the local chiral field formed drove a specific structural assembly of AuNRs within the components, thereby leading to the formation of CGNAs.

There are some reports about small chiral molecules as connections to form CGNAs for the sensitive detection of amino acids or peptides [68]. The method utilizing Cys or GSH molecules' preferential adsorb at the end of AuNRs to obtain end-to-end chiral components can be used for enantiomeric identification/detection based on the dose-dependent PCD reaction (Fig. 4a). Additionally, Song et al. [69] found that the environmental molecular can serve as a chiral dynamic template to facilitate the construction of CGNAs (Fig. 4b), which was a novel chiral small molecule linker mode that innovatively combined dynamic chiral templates. The AuNPs were located in a molecular environment composed of hexadecyltrimethylammonium bromide (CTAB), citrate and Cys, and a "majority rule" effect was observed during the formation of the superstructure, where a number of matrix molecules compete for the surface binding sites of the particles due to charge interactions, thus acting as a dynamic template to constrain the surface chiral molecules of the particles and affecting the chiral arrangement and assembly of the particles.

Common biomolecules could serve as chiral drivers or connectors for nanostructures, including DNA/RNA, proteins, or peptides. Xu et al. [70] constructed DNA driven gold heterodimers, which exhibited significant chiral optical activity in the visible light region. The dimer is composed of two kinds of metal NPs: one functionalized with telomerase primers, and the other coupled with complementary linker sequences. These NPs are connected by the DNA linker. In the presence of telomerase, the dimer structure is disrupted, and the separation of chiral assemblies leads to a decrease in the CD signal. Therefore, it can be used for quantitative detection of telomerase activity in cells. The inherent chirality of proteins/peptides plays a guiding role in the stereochemical configuration of NPs during self-assembly, strongly affecting the growth of chiral nanostructures. While the construction of chiral drivers or ligands for protein/peptide can also be achieved through NPs assembly with antibody-antigen specific biorecognition principles [71].

Interestingly, the electrostatic interactions between proteins and AuNPs can also be used to construct chiral superstructures. Wang et al. [72] demonstrated that human serum albumin (HSA) and porcine serum albumin (PSA) could guide the chiral assembly of AuNRs (Fig. 4c), and their left-handed optical response was opposite to a series of other homologous animal serum albumin due to their different surface charge distributions. Under physiological pH conditions, the assembly of HSA or PSA with AuNRs produced

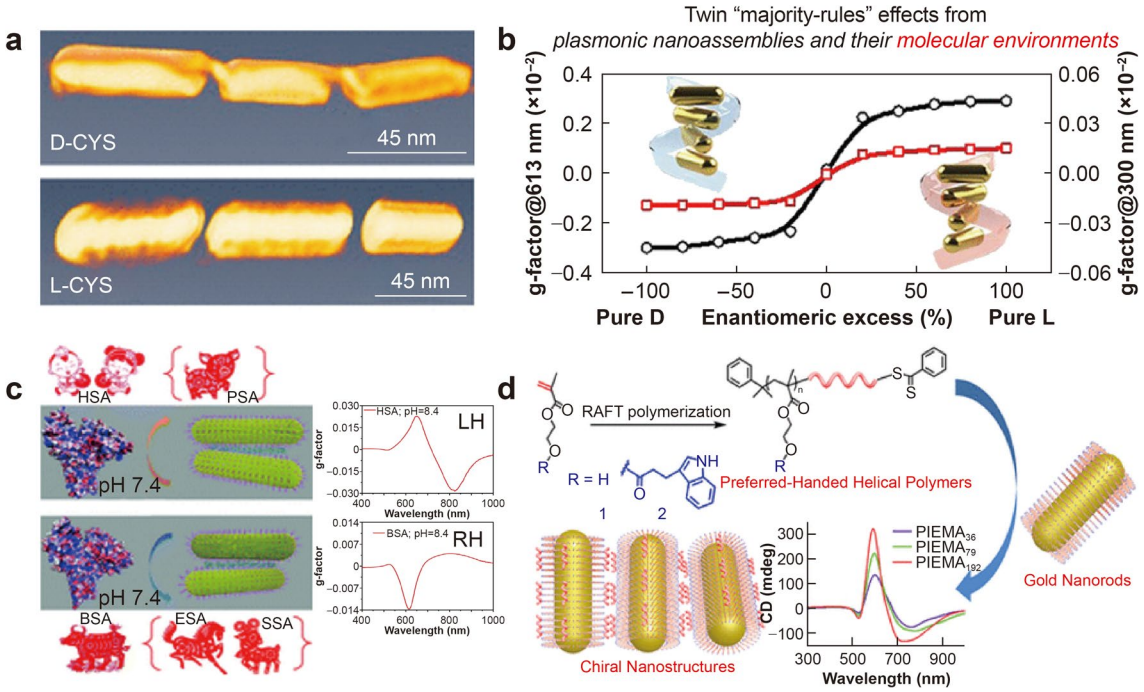

Fig. 4 Gold chiral superstructures self-assembled by chiral linkers. **a** The chiral gold nanostructures linked by Cys (Reprinted with permission from Ref. [68]. Copyright © 2015 American Chemical Society). **b** Helical assemblies of gold nanorods driven by Cys and environment (Reprinted with permission from Ref. [69]. Copyright © 2021 American Chemical Society). **c** The gold nanostructures linked by protein fibers (Reprinted with permission from Ref. [72]. Copyright © 2021 Royal Society of Chemistry). **d** The gold nanostructures linked by chiral polymers (Reprinted with permission from Ref. [73]. Copyright © 2019 American Chemical Society)

left-handed twisted aggregates, while bovine serum albumin (BSA), sheep serum albumin (SSA), and horse serum albumin (ESA) were the opposite. The driving force of chiral assembly was mainly attributed to electrostatic interactions. The obtained opposite chiral optical signals were correlated with the chiral surface charge distribution of the serum albumin tertiary structure.

In addition to small chiral molecules and biomolecules, the synthesis of chiral polymers also shows promising prospects in constructing chiral plasmonic superstructure. For example, Liu et al. [73] prepared molecules of hydroxyethyl methacrylate 3-indole propionate with different degrees of polymerization to investigate the chain transfer polymerization. By using them as connectors for AuNRs, chiral assemblies were obtained (Fig. 4d), and the tilt of AuNRs within this superstructure was the origin of PCD response. In addition to artificial chiral polymers, oligomers formed by self-assembly of some small biomolecules can also serve as chiral linkers to assemble AuNPs into chiral supramolecules. For example, GSH can form helical GSH oligomers in the hydrophobic core of CTAB micelles, and spiral GSH oligomers lead to chiral and end-to-end cross assembly of nanorods [74].

3.2 Chiral Templates

There are many types of chiral templates, which could be achieved by depositing NPs on these templates and arranging them into a certain chiral assembly. A multitude of chiral macromolecules or superstructures serve as chiral templates. Among them, DNA origami is one of the most widely used techniques for manufacturing chiral superstructures with high level of spatial accuracy and programmable nanostructure, which can endow AuNPs with flexible functional sites. In this case, the bottom-up assembly of nanostructures can generate new physical and chemical properties [27]. Since the technology was introduced in 2012 for customizing chiral plasmonic components for optical response, most of the chiral gold nanocomponents are constructed with non-chiral AuNPs to obtain structural chirality [75, 76]. For instance, Kevin et al. [77] employed DNA origami to assemble multiple AuNPs into helical CGNAs (Fig. 5a). By meticulously locating CGNAs in space and observing the impact of the geometric shape of the reconstructed superstructure on its surrounding optical near-field, they gained valuable insights into the underlying mechanisms governing the optical properties of these structures. The model revealed previously undiscovered chiral plasmon dielectric coupling phenomena, which explained the complex electromagnetic interactions and resonance hotspots in plasmonic nanostructures based on the mixed DNA. This was beneficial for the analysis and understanding of interactions between chiral components and natural molecules.

In recent years, DNA origami technology has been used to construct CGNAs to investigate the relationship between the structural chirality of superstructures and the inherent chirality of individual particles. For example, Pan et al. [78] designed two different modes of DNA folding boards and assembled four sets of single particles, including two HPNRs with the same chirality and two HPNRs with opposite chirality, chiral HPNRs with non-chiral AuNRs, and two non-chiral AuNRs, to obtain several different chiral dimer superstructures (Fig. 5b), exploring the relationship between inherent chirality and structurally coupled chirality in chiral supramolecular structures, and have obtained a chiral supramolecule much stronger than that formed by coupling non-chiral AuNPs.

Chiral templates, as a synthetic method for chiral gold nanostructures, present a variety of types. The chiral plasmonic superstructure constructed with templates offer many advantages, such as high stability and flexible design. By deposition and chiral assembly of AuNPs with peptides or proteins as templates, the chiral superstructure could be obtained [79, 80]. For example, Lu et al. [30] used human pancreatic amyloid like protein peptides (hIAPPs) as templates to self-assemble AuNRs into helical fibers. As a consequence of the long-range order of the superstructure, a chiral plasmonic superstructure with extremely strong PCD signals (g-factor of 0.12) can be obtained (Fig. 5c). Compared with a single AuNRs covered with peptides, the g-factor is increased by thousands of times due to the significant spectral shift under circularly polarized photons and reduced scattering of energy states when dipoles are oriented in an antiparallel manner. In addition, there are polymer templates and environmental matrix templates. For example, Lu et al. [81] used self-assembly of D/L type tartaric acid (TA) to guide non-chiral self-assembly of achiral poly(1,4-butadiene)-*b*-poly(ethylene oxide) cross-linked block copolymer (BCP) into pores with specified chirality and helical morphology. Subsequently, the chiral optical response was demonstrated by arranging AuNPs spirals (Fig. 5d). Discovering the spiral structure and chirality of the array only requires adjusting the D/L porous template, which provides a convenient and fast way to prepare chiral porous BCP films and spiral NPs arrays.

3.3 Chiral Light Induced Nanoscale Gold Superstructures

Photon-induced chiral transfer provides a simple and universal method for chiral system. Due to the strong rotational ability of highly delocalized plasmonic states, plasmonic NPs are promising candidates for chiral light induced

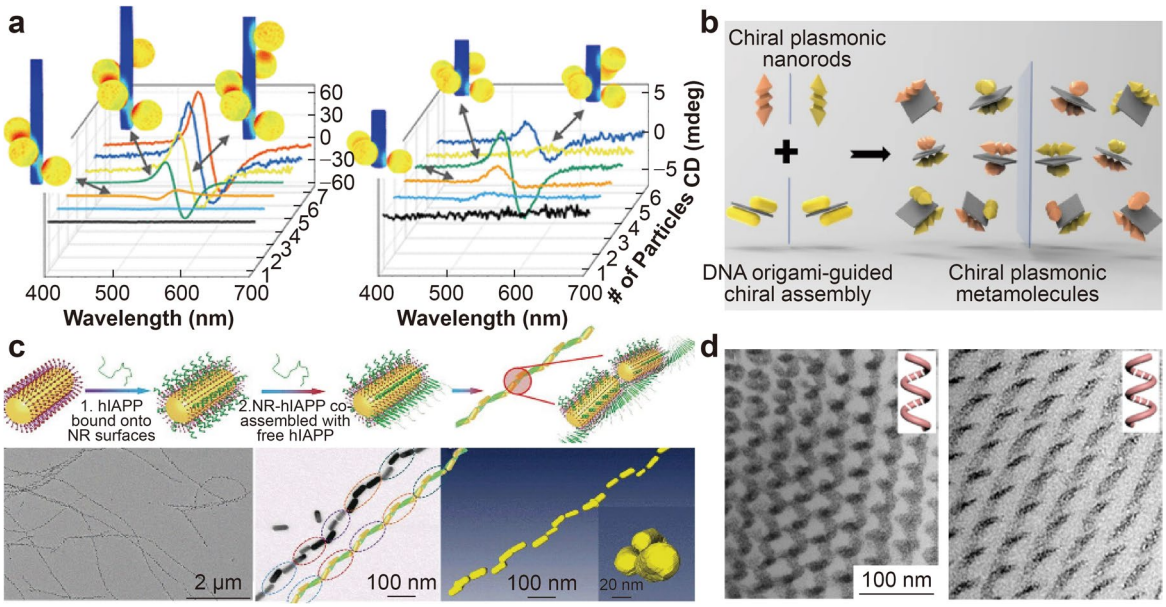

Fig. 5 Schematic diagram of CGNAs induced by chiral templates. **a** Chiral superstructure constructed by chiral AuNPs (Reprinted with permission from Ref. [77] Copyright © 2022 American Chemical Society). **b** Schematic diagram of the construction of chiral gold nanorods dimers (Reprinted with permission from Ref. [78] Copyright © 2022 Tsinghua University Press). **c** The formation of hIAPPs-AuNRs helical superstructures (Reprinted with permission from Ref. [30] Copyright © 2021 American Association for the Advancement of Science) [30]. **d** BCP-mediated helical gold nanostructures (Reprinted with permission from Ref. [81] Copyright © 2017 American Chemical Society)

preparation. However, due to the short lifetime of plasmonic states, this method is more challenging for plasmonic NPs than semiconductors. Previously, Zhu et al. [82] achieved the formation of light-induced chiral gold nanoaggregates from an alternative perspective. They perturbed the ordered arrangement of the superstructure and then used ultraviolet light as a triggering condition for the self-assembly of supramolecular chiral materials to achieve light induction of the chiral gold nanosuperstructures. Despite some challenges, the advantages of metal NPs make photon-induced chiral transfer possible. For example, Kim et al. [65] induced the formation of AuNPs by irradiating $HAuCl_4$ solution with circularly polarized light, and then assembled them into chiral nanostructures with a diameter of 10–15 nm (Fig. 6). Despite their seemingly irregular shapes, the resulting colloids exhibited CD spectra with opposite polarity when exposed to photons with left and right CPL. Considering the existing large number of different discrete plasmonic NPs, similar synthesis schemes based on light induction can be applied to other discrete NPs that can spontaneously assemble into upper structures with a lattice-to-lattice connections. By optimizing the power of incident light and the interactions between NPs-NPs, nanoscale chiral components with more uniform shapes can be prepared.

4 The Biosensing Platforms with Chiral Gold Nanomaterials

Owing to the unique property, chiral gold nanomaterials have found wide applications in biosensing [69–72] and cancer treatments [83], and so on [84]. Furthermore, the various biosensing platforms could be developed based on different optical properties, including absorption, surface-enhanced Raman scattering (SERS), dark-field light scattering, circular dichroism spectra, and so forth.

Prior to the advent of intrinsic chiral AuNPs, the principal biosensing applications of chiral gold nanomaterials were AuNAs and core–shell chiral NPs. Among these, the biosensing applications of chiral assemblies primarily employ chiral biological components to induce the formation or separation of assemblies [1], as well as the near-field or hotspot interactions between already formed chiral assemblies and biological components [85]. Regarding the former, Li' Group [86] reported the visual differentiation between the L- and D-forms of mandelic acid (MA), which was based on the chirality of L-tartaric acid (L-TA)-capped AuNPs. And the visual differentiation can be used as chiral selector for MA. The color of L-TA-capped AuNPs changed from red to blue upon the addition of L-MA, whereas no color change could be observed when D-MA was

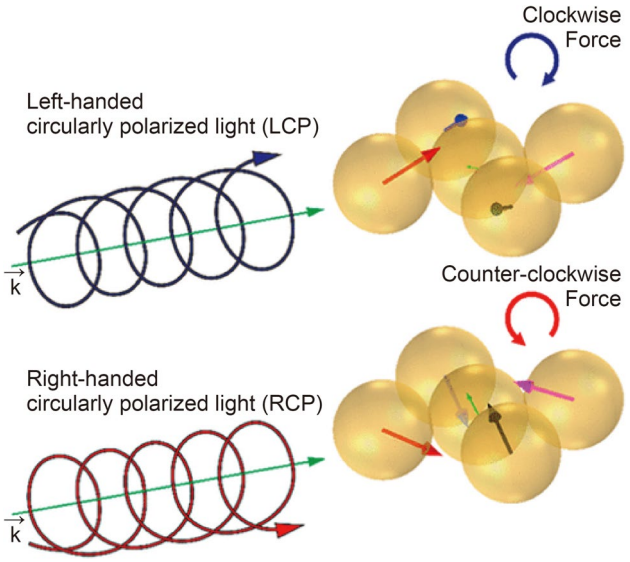

Fig. 6 Gold superstructure shape driven by CPL illumination (Reprinted with permission from Ref. [65] Copyright © 2019 American Chemical Society)

added. The proposed chiral assay can be observed with naked eyes and quantified by spectrophotometry, not requiring complicated chiral modification (Fig. 7a). A CD biosensor for major shellfish allergen tropomyosin (TROP) was developed based on a chiral assembly of polymer of AuNP trimers (Fig. 7b) [87]. In that work, TROP and anti-TROP monoclonalantibodies (mAb) were immobilized on 20 nm and 30 nm 16-mercaptohexadecanoic acid (16-MHDA) functionalized AuNPs to assemble a trimer, which present a strong CD signal. The free TROP from samples was quantified as an inhibitor for the formation of the AuNP trimer, leading to the specific and accurate reduction of CD signal. With regard to the latter, extensive research has been conducted on the near-field biosensing of chiral assemblies [49, 86]. Yuanhai et al. [48] utilized non chiral gold nanocubes arranged in a planar "τ"-shaped structure array, which exhibited a great CD signal and enhanced hyperchiral field, and a conformal array was used to achieve ultra-sensitive detection of single molecule BSA protein (Fig. 7c).

The explosive growth of inherently chiral AuNPs in recent years has led to the development of promising new materials for biosensing applications. The excellent chiral and surface plasmon properties, as well as the superior surface chemical properties brought by chiral morphology, make these materials highly promising for biosensing applications [88]. The chiral near-field and hotspots on the surface of inherent chiral materials, as well as their selective resonance coupling with enantiomeric dipoles, give them great advantages in biological enantiomer recognition [89, 90]. A multitude of intrinsic chiral materials have been employed for chiral recognition leveraging their chiral near-field [91]. Wu et al. [51] exploited the chiral near-field to demonstrate enantiomeric electrochemical enhanced asymmetry, and performed plasmon-enhanced electrochemical recognition of pen enantiomers by synthesizing chiral hotspots with inherent chiral gold cubic surface folds (Fig. 7d). And Xu's Group [92] developed L/D-Pt@Au triangular nanorings (TNRs) with strong optical activity, which can be effectively used for the discrimination of enantiomers due to selective resonance coupling between the induced electric and magnetic dipoles associated with enantiomers and the chiral plasmonic TNRs, also known as the surface-enhanced Raman scattering-chiral anisotropy (ChA) effect. The chiral D-Pt@Au TNRs represented a label-free SERS platform that can be applied to detect Aβ monomers and fibrils. In addition, chiral D-Pt@Au TNRs can also successfully detect Aβ42 proteins in Alzheimer's disease (AD) patients with high sensitivity, opening up an avenue for early diagnosis of protein-misfolding diseases with chiral plasmonic nanomaterials as ultrasensitive SERS substrates (Fig. 7e). Additionally, chiral Au nanotriangles (c-AuNTs) in the form of propellers have been employed as SERS substrates with notable success in the detection and differentiation of biological components, including levodopa, doxorubicin (DOX), levo/D-carnitine [23], and GNAs previously mentioned that recognize Fmoc-L/D-phenylalanine (Fmoc-L/D-Phe) through Raman signals [24].

The above approaches are based on the intrinsic characteristics of the materials and have made significant progress in the recognition of biological enantiomers. Given the three major strategies for quantitative detection of plasmonic nanomaterials, namely growth, aggregation/disaggregation and etching, it is hypothesized that intrinsic chiral gold nanomaterials may be able to generate more sensitive signal changes using these strategies. With regard to growth strategies, anisotropic growth has been extensively employed for the identification of biological components [52]. However, no further applications of isotropic growth have been identified to date. Some research groups have attempted to assemble or disassembled chiral particles, including HPNRs DNA origami dimer [78] and Sonia's controlled assembly of a dog bone-shaped chiral gold nanostructure [39], which helps to tune and enhance chiral signals. Regrettably, none of these structures have been utilized for biosensing purposes. Finally, there is a paucity of research on the etching of inherently chiral materials. The inherent chirality and localized surface plasmon resonance properties of AuNPs are highly correlated with particles' morphology.

Furthermore, the inherent chiral nature of AuNPs results in most of them having irregular surfaces and sharp surface protrusions. This also leads to more diverse signal changes in intrinsic CGNPs etching, far exceeding those of non-chiral AuNPs. For that, our group developed an innovative and sensitive biosensor for hepatitis B virus (HBV)-DNA detection based on the surface etching of the helical gold nanorods

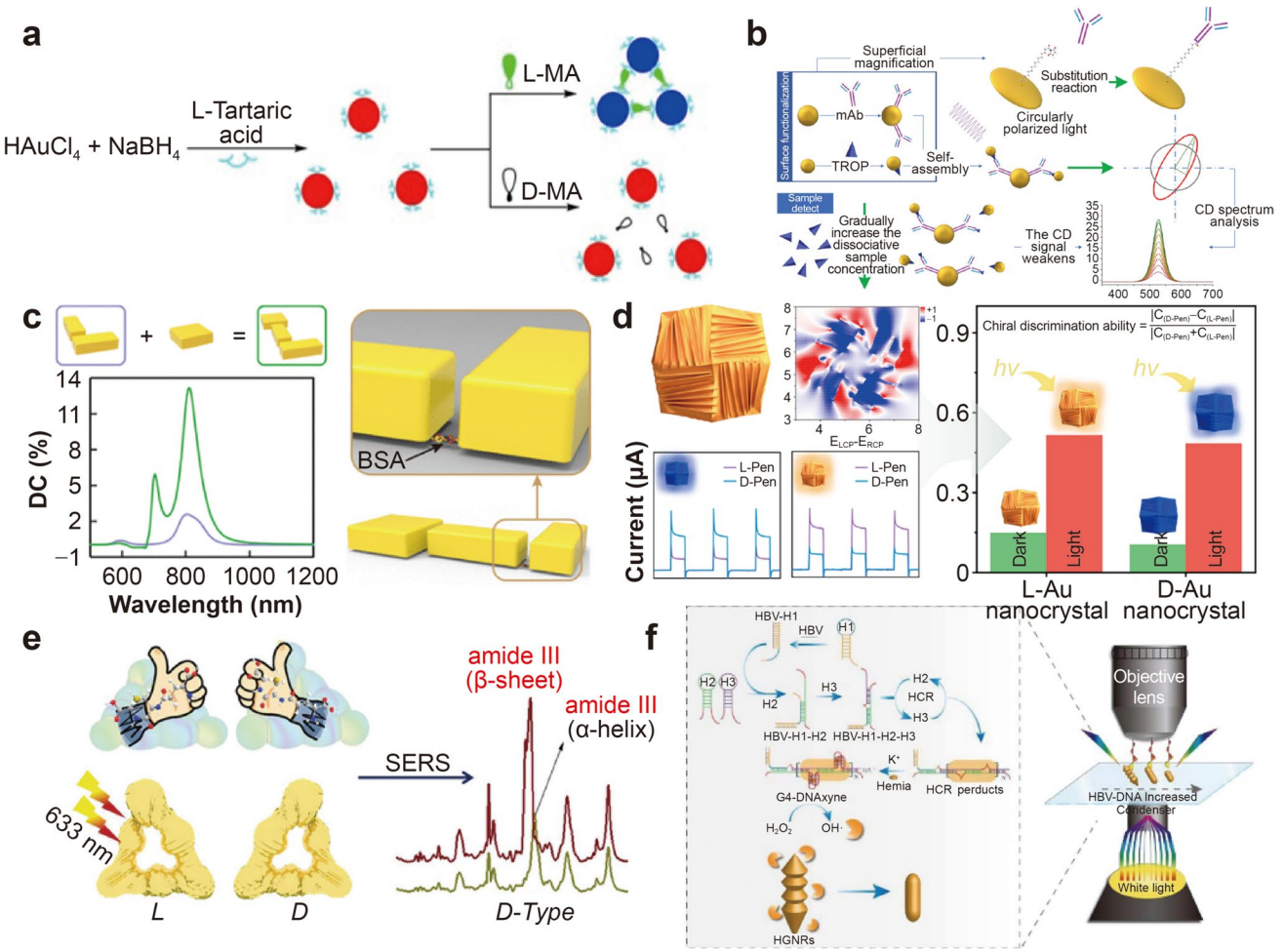

Fig. 7 The biosensing platforms with chiral gold nanomaterials. **a** Visual chiral recognition of mandelic acid enantiomers with L-tartaric acid-capped AuNPs as colorimetric probes (Reprinted with permission from Ref. [86] Copyright © 2015 Elsevier Ltd.). **b** Schematic illustration for the AuNPs trimer based biosensor for TROP detection (Reprinted with permission from Ref. [87] Copyright © 2019 Elsevier Ltd.). **c** Ultra-sensitive detection of BSA using gold nano chiral array (Reprinted with permission from Ref. [48] Copyright © 2022 American Chemical Society). **d** Intrinsic chiral nanogold cube to recognize Fmoc-L/D-phenylalanine (Reprinted with permission from Ref. [51] Copyright © 2023 American Chemical Society). **e** Chiral plasmonic triangular nanorings for ultrasensitive detection of amyloid proteins in Alzheimer's disease (Reprinted with permission from Ref. [92] Copyright © 2021 WILEY–VCH Verlag GmbH & Co. KGaA, Weinheim). **f** Schematic diagram of highly sensitive detection strategy for HBV-DNA based on surface etching of the helical gold nanorods (Reprinted with permission from Ref. [14] Copyright © 2023 Elsevier Ltd.)

(HGNRs) at a single-particle level under a dark-field microscope (DFM). Herein, the unique HGNRs with high surface activity were functionalized as the optical probe, which were etched to the smooth gold nanorods and even to gold nanospheres, resulting in a distinct color and light scattering change of single particle, as well as the disappearance of CD optical properties (Fig. 7f) [14].

5 Summary and Outlook

In the past decades, chiral plasmonic nanomaterials have developed rapidly, which could be constructed with chiral molecules as connectors to provide chiral driving force to form chiral assemblies, or by forming asymmetric adsorption configurations on chiral templates/media. These chiral gold nanomaterials obtained through self-assembly of chiral or non-chiral AuNPs exhibit strong plasmonic chirality. Based on the dynamic reversibility, researchers have developed simple, fast, and real-time chiral control systems that can generate chiral conformational changes and PCD response changes to various external stimuli. However, there are still challenges in making AuNPs more precisely arranged on chiral templates or connections and clarifying the chirality patterns in superstructures more clearly.

In recent years, with the development of wet chemical synthesis technology, more CGNPs with clear chiral 3D morphology and strong plasmonic chiral response can be

obtained through seeds-regrowth methods. This provides favorable research conditions for exploring the origin of chirality and utilizing chiral nanomaterials for biomedical, physical and chemical applications. So far, the frequently reported chiral ligand is small molecule Cys. The utilization of diverse theoretical simulations for the screening of efficient chiral-induced thiols can facilitate the selection and rational design of appropriate chiral ligands. In addition to the strong thiol ligands, the cosurfactants of weak ligands and chiral light irradiation also display hand-growth inducing effects. Further detailed mechanism research is required to establish a theoretical basis for the precise regulation of the chiral morphology.

The development of chiral AuNPs has made significant progress. Considering to achieve the applications of these material structures, many theoretical foundations and technical challenges are still needed to address in the coming years. Basic theoretical research, such as the developing multi-scale layered chirality concept, elucidating the molecular mechanisms, theoretical models, and biological similarities involved in the optical processes, chemical reactions, and biological effects of chiral nanoparticles based on this concept. This may require interdisciplinary collaboration among researchers in physics, chemistry, materials, and biochemistry fields. Another technical challenge is how to simultaneously preserve high g-factor and other optical parameters during the transition of chiral nanomaterials synthesis program from laboratory to factory. In summary, there are both opportunities and challenges in the research of chiral plasmonic nanomaterials which have significant research significance in catalysis, biology, medicine, biotechnology, nonlinear optics, photonics, and quantum effects.

Acknowledgements This research was funded by the National Natural Science Foundation of China (22174115), the research grant from Shangqiu Medical College (KFKT2303), as well as the Innovation and Entrepreneurship Project of Southwest University (S202310635341).

Data availability The data that support the findings of this study are available on request from the corresponding author. The data are not publicly available due to privacy or ethical restrictions.

Declarations

Conflict of interest The authors declare that they have no conflict of interests.

References

1. Zhang QF, Hernandez T, Smith KW, Jebeli SAH, Dai AX, Warning L, Baiyasi R, McCarthy LA, Guo H, Chen DH, Dionne JA, Landes CF, Link S. Unraveling the origin of chirality from plasmonic nanoparticle-protein complexes. Science. 2019;365:1475–8.
2. Lee HE, Kim RM, Ahn HY, Lee YY, Byun GH, Im SW, Mun J, Rho J, Nam KT. Cysteine-encoded chirality evolution in plasmonic rhombic dodecahedral gold nanoparticles. Nat Commun. 2020;11:263.
3. Li Y, Jin XN, Cheng Y, Ma XF, Wang Y. Recent advances on chiral mobile phase additives: a critical review. J Anal Test. 2022;6:129–62.
4. Chen Y, Ma W. The origin of biological homochirality along with the origin of life. PLoS Comput Biol. 2020;16: e1007592.
5. John N, Mariamma AT. Recent developments in the chiroptical properties of chiral plasmonic gold nanostructures: bioanalytical applications. Microchim Acta. 2021;188:424.
6. Wen T, Li JY, Cai WR, Yang BZ, Kong Y, Yin ZZ. A chiral sensing platform based on a multi-substituted ferrocene-cuprous ion complex for the discrimination of electroactive amino acid isomers. Analyst. 2023;148:919–25.
7. Li HB, Gao XS, Zhang CQ, Ji YL, Hu ZJ, Wu XC. Gold-nanoparticle-based chiral plasmonic nanostructures and their biomedical applications. Biosensors. 2022;12:957.
8. Yang F, Wang M, Zhang DQ, Yang J, Zheng M, Li Y. Chirality pure carbon nanotubes: growth, sorting, and characterization. Chem Rev. 2020;120:2693–758.
9. Diehl F, Hageneder S, Fossati S, Auer SK, Dostalek J, Jonas U. Plasmonic nanomaterials with responsive polymer hydrogels for sensing and actuation. Chem Soc Rev. 2022;51:3926–63.
10. Choi KH, Lee HJ, Park BJ, Wang KK, Shin EP, Park JC, Kim YK, Oh MK, Kim YR. Photosensitizer and vancomycin-conjugated novel multifunctional magnetic particles as photoinactivation agents for selective killing of pathogenic bacteria. Chem Commun. 2012;48:4591–3.
11. Chen Y, Zheng J, Zhang L, Li S, Chen Y, Chui KK, Zhang W, Shao L, Wang J. Inversion of the chiroptical responses of chiral gold nanoparticles with a gold film. ACS Nano. 2024;18:383–94.
12. Wang J, Zhang P, Li CM, Li YF, Huang CZ. A highly selective and colorimetric assay of lysine by molecular-driven gold nanorods assembly. Biosens Bioelectron. 2012;34:197–201.
13. Liu JJ, Wen S, Yan HH, Cheng R, Zhu F, Gao PF, Zou HY, Huang CZ, Wang J. The accurate imaging of collective gold nanorods with a polarization-dependent dark-field light scattering microscope. Anal Chem. 2023;95:1169–75.
14. Cheng R, Li LT, Huang M, Zhu F, Li Q, Liu H, Gao J, Zhao XH, Luo FK, Wang J. Highly sensitive plasmonic biosensor for hepatitis B virus DNA based on the surface etching of the active helical gold nanorods. Chem Eng J. 2023;468: 143627.
15. Zhang Q, Yan HH, Ru C, Zhu F, Zou HY, Gao PF, Huang CZ, Wang J. Plasmonic biosensor for the highly sensitive detection of microRNA-21 via the chemical etching of gold nanorods under a dark-field microscope. Biosens Bioelectron. 2022;201: 113942.
16. Yan HH, Zhang Q, Cheng R, Zhu F, Liu JJ, Gao PF, Zou HY, Liang GL, Huang CZ, Wang J. Size-dependent plasmonic resonance scattering characteristics of gold nanorods for highly sensitive detection of microRNA-27a. ACS Appl Bio Mater. 2021;4:3469–75.
17. Liu JJ, Yan HH, Zhang Q, Gao PF, Li CM, Liang GL, Huang CZ, Wang J. High-resolution vertical polarization excited dark-field microscopic imaging of anisotropic gold nanorods for the sensitive detection and spatial imaging of intracellular microRNA-21. Anal Chem. 2020;92:13118–25.
18. Zhang HZ, Li RS, Gao PF, Wang N, Lei G, Huang CZ, Wang J. Real-time dark-field light scattering imaging to monitor the coupling reaction with gold nanorods as an optical probe. Nanoscale. 2017;9:3568–75.
19. Cai ZX, Chen YZ, Meteku BE, Zheng QW, Li FM, Zhang MS, Zeng JB, Chen X. Cu^{2+}-assisted synthesis of Au@AgI core/shell nanorods via in situ oxidation of iodide: A strategy for colorimetric iodide sensing. J Anal Test. 2022;6:374–81.

20. Jing L, Xie CY, Li QQ, Yao HF, Yang MQ, Li H, Xia F, Li SG. A sandwich-type lateral flow strip using a split, single aptamer for point-of-care detection of cocaine. J Anal Test. 2022;6:120–8.
21. Fan ZY, Govorov AO. Plasmonic circular dichroism of chiral metal nanoparticle assemblies. Nano Lett. 2010;10:2580–7.
22. Miandashti AR, Khorashad LK, Kordesch ME, Govorov AO, Richardson HH. Experimental and theoretical observation of photothermal chirality in gold nanoparticle helicoids. ACS Nano. 2020;14:4188–95.
23. Ma YJ, Cao ZZ, Hao JJ, Zhou JH, Yang ZJ, Yang YZ, Wei JJ. Controlled synthesis of Au chiral propellers from seeded growth of Au nanoplates for chiral differentiation of biomolecules. J Phys Chem C. 2020;124:24306–14.
24. Wen X, Wang S, Liu RL, Duan R, Hu S, Jiao TF, Zhang L, Liu MH. Selenocystine and photo-irradiation directed growth of helically grooved gold nanoarrows. Small. 2022;18:2104301.
25. Wu FX, Tian Y, Luan XX, Lv XL, Li FH, Xu GB, Niu WX. Synthesis of chiral Au nanocrystals with precise homochiral facets for enantioselective surface chemistry. Nano Lett. 2022;22:2915–22.
26. Huang YK, Nguyen MK, Natarajan AK, Nguyen VH, Kuzyk A. A DNA origami-based chiral plasmonic sensing device. ACS Appl Mater Interfaces. 2018;10:44221–5.
27. Zhao L, Zhou Y, Niu GM, Gao FC, Sun ZW, Li H, Jiang YY. Advances in chiral gold nano-assemblies and their bioapplication based on optical properties. Part Part Syst Char. 2022;39:2100231.
28. Sun MZ, Qu AH, Hao CL, Wu XL, Xu LG, Xu CL, Kuang H. Chiral upconversion heterodimers for quantitative analysis and bioimaging of antibiotic-resistant bacteria in vivo. Adv Mater. 2018;30:1804241.
29. Miao PD, Xi Y, Feng ZJ, Zhang J, Du YX, Chen C. Enhanced enantioseparation of drugs by capillary electrochromatography with a L-cysteine functionalized gold nanoparticle based stationary phase. Anal Methods. 2022;14:1982–7.
30. Lu J, Xue Y, Bernardino K, Zhang NN, Gomes WR, Ramesar NS, Liu SH, Hu Z, Sun TM, de Moura AF, Kotov NA, Liu K. Enhanced optical asymmetry in supramolecular chiroplasmonic assemblies with long-range order. Science. 2021;371:1368–74.
31. Hou K, Zhao J, Wang H, Li B, Li K, Shi X, Wan K, Ai J, Lv J, Wang D, Huang Q, Wang H, Cao Q, Liu S, Tang Z. Chiral gold nanoparticles enantioselectively rescue memory deficits in a mouse model of Alzheimer's disease. Nat Commun. 2020;11:4790.
32. Kang X, Wang Y, Cai XL, Hua Y, Shao ZH, Chen XY, Zhao XL, Zang SQ. Chiral gold clusters functionalized two-dimensional nanoparticle films to regulate the adhesion and differentiation of stem cells. J Colloid Interface Sci. 2022;625:831–8.
33. Ahn J, Ma S, Kim JY, Kyhm J, Yang W, Lim JA, Kotov NA, Moon J. Chiral 2D organic inorganic hybrid perovskite with circular dichroism tunable over wide wavelength range. J Am Chem Soc. 2020;142:4206–12.
34. Hu ZJ, Meng DJ, Lin F, Zhu X, Fang ZY, Wu XC. Plasmonic circular dichroism of gold nanoparticle based nanostructures. Adv Opt Mater. 2019;7:1801590.
35. Li JH, Li XK, Feng J, Yao W, Zhang H, Lu CJ, Liu RR. Organocatalytic enantioselective synthesis of seven-membered ring with inherent chirality. Angew Chem Int Ed. 2024;63: e202319289.
36. Majoinen J, Hassinen J, Haataja JS, Rekola HT, Kontturi E, Kostiainen MA, Ras RHA, Törmä P, Ikkala O. Chiral plasmonics using twisting along cellulose nanocrystals as a template for gold nanoparticles. Adv Mater. 2016;28:5262–7.
37. Ben-Moshe A, Maoz B, Govorov AO, Markovich G. Chirality and chiroptical effects in inorganic nanocrystal systems with plasmon and exciton resonances. Chem Soc Rev. 2013;42:7028–41.
38. Chen Z, Lu XY. Self-assembly of plasmonic chiral superstructures with intense chiroptical activity. Nano Express. 2024;3:32002.
39. Maniappan S, Dutta C, Solís DM, Taboada JM, Kumar J. Surfactant directed synthesis of intrinsically chiral plasmonic nanostructures and precise tuning of their optical activity through controlled self-assembly. Angew Chem Int Ed. 2023;135: e202300461.
40. Chopra H, Bibi S, Singh I, Hasan MM, Khan MS, Yousafi Q, Baig AA, Rahman MM, Islam F, Emran TB, Cavalu S. Green metallic nanoparticles: biosynthesis to applications. Front Bioeng Biotech. 2022;10: 874742.
41. Sahu BK, Dwivedi A, Pal KK, Pandian R, Dhara S, Das A. Optimized Au NRs for efficient SERS and SERRS performances with molecular and longitudinal surface plasmon resonance. Appl Surf Sci. 2021;537: 147615.
42. Lee S, Fan C, Movsesyan A, Bürger J, Wendisch FJ, Menezes LDS, Maier SA, Ren H, Liedl T, Besteiro LV, Govorov AO, Cortés E. Unraveling the chirality transfer from circularly polarized light to single plasmonic nanoparticles. Angew Chem Int Ed. 2024;63:202319920.
43. Liu W, Zhu Z, Deng K, Li Z, Zhou Y, Qiu H, Gao Y, Che S, Tang Z. Gold nanorod@chiral mesoporous silica core–shell nanoparticles with unique optical properties. J Am Chem Soc. 2013;135:9659–64.
44. Azizi A, Ranjbar B, Moghadam TT, Bagheri Z, Baglou SR. Surface plasmon resonance coupled circular dichroism of DNA-gold nanorods assembly. J Phys D Appl Phys. 2014;47: 315401.
45. Zheng GC, Rao ZY, Pérez-Juste J, Du RL, Liu W, Dai JY, Zhang W, Lee LYS, Wong KY. Tuning the morphology and chiroptical properties of discrete gold nanorods with amino acids. Angew Chem Int Ed. 2018;57:16452–7.
46. Yan J, Chen YD, Hou S, Chen JQ, Meng DJ, Zhang H, Fan HZ, Ji YL, Wu XC. Fabricating chiroptical starfruit-like Au nanoparticles *via* interface modulation of chiral thiols. Nanoscale. 2017;9:11093–102.
47. Meng DJ, Li X, Gao XS, Zhang CQ, Ji YL, Hu ZJ, Ren LL, Wu XC. Constructing chiral gold nanorod oligomers using a spatially separated sergeants-and-soldiers effect. Nanoscale. 2021;13:9678–85.
48. Lin Y, Che D, Guo H, Wang J. Strong near-field coupling for enhancing plasmonic chirality toward single-molecule sensing. J Phys Chem C. 2022;126:14750–7.
49. Niinomi H, Sugiyama T, Cheng A-C, Tagawa M, Ujihara T, Yoshikawa HY, Kawamura R, Nozawa J, Okada JT, Uda S. Chiral optical force generated by a superchiral near-field of a plasmonic triangle trimer as origin of giant bias in chiral nucleation: a simulation study. J Phys Chem C. 2021;125:6209–21.
50. Wang Z, Teh BH, Wang Y, Adamo G, Teng J, Sun H. Enhancing circular dichroism by super chiral hot spots from a chiral metasurface with apexes. Appl Phys Lett. 2017;110: 221108.
51. Wu F, Li F, Tian Y, Lv X, Luan X, Xu G, Niu W. Surface topographical engineering of chiral Au nanocrystals with chiral hot spots for plasmon-enhanced chiral discrimination. Nano Lett. 2023;23:8233–40.
52. Lee HE, Ahn HY, Mun J, Lee YY, Kim M, Cho NH, Chang K, Kim WS, Rho J, Nam KT. Amino-acid- and peptide-directed synthesis of chiral plasmonic gold nanoparticles. Nature. 2018;556:360–5.
53. Chen JQ, Gao XS, Zheng Q, Liu JB, Meng DJ, Li HY, Cai R, Fan HZ, Ji YL, Wu XC. Bottom-up synthesis of helical plasmonic nanorods and their application in generating circularly polarized luminescence. ACS Nano. 2021;15:15114–22.
54. Chen JQ, Li HB, Lu X, Liu XY, Feng W, Wang P, Zhao JQ, Zhu ZY, Zheng GC, Wu XC. Two-thiols-regulated fabrication of plasmonic nanoparticles with co-enhanced Raman scattering and circular dichroism responses. Rare Met. 2023;42:3673–81.

55. Gao X, Zheng Q, Li H, Zhang C, Cai R, Ji Y, Hu Z, Wu X. Modulation of plasmonic chiral shell growth on gold nanorods via non-chiral surfactants. Nanoscale. 2023;15:10651–60.
56. Zhang NN, Sun HR, Liu S, Xing YC, Lu J, Peng F, Han CL, Wei Z, Sun T, Yang B, Liu K. Gold nanoparticle enantiomers and their chiral-morphology dependence of cellular uptake. CCS Chem. 2022;4:660–70.
57. Ni B, Mychinko M, Gomez-Grana S, Morales-Vidal J, Obelleiro-Liz M, Heyvaert W, Vila-Liarte D, Zhuo X, Albrecht W, Zheng G, Gonzalez-Rubio G, Taboada JM, Obelleiro F, Lopez N, Perez-Juste J. Chiral seeded growth of gold nanorods into fourfold twisted nanoparticles with plasmonic optical activity. Adv Mater. 2023;35: e2312066.
58. Zheng J, Boukouvala C, Lewis GR, Ma Y, Chen Y, Ringe E, Shao L, Huang Z, Wang J. Halide-assisted differential growth of chiral nanoparticles with threefold rotational symmetry. Nat Commun. 2023;14:3783.
59. Zheng Y, Li X, Huang L, Li X, Yang S, Wang Q, Du J, Wang Y, Ding W, Gao B, Chen H. Homochiral nanopropeller via chiral active surface growth. J Am Chem Soc. 2023;146:410–8.
60. Gonzalez-Rubio G, Mosquera J, Kumar V, Pedrazo-Tardajos A, Llombart P, Solis DM, Lobato I, Noya EG, Guerrero-Martinez A, Taboada JM, Obelleiro F, MacDowell LG, Bals S, Liz-Marzan LM. Micelle-directed chiral seeded growth on anisotropic gold nanocrystals. Science. 2020;368:1472–7.
61. Cho NH, Kim YB, Lee YY, Im SW, Kim RM, Kim JW, Namgung SD, Lee H-E, Kim H, Han JH, Chung HW, Lee YH, Han JW, Nam KT. Adenine oligomer directed synthesis of chiral gold nanoparticles. Nat Commun. 2022;13:3831.
62. Xu L, Wang X, Wang W, Sun M, Choi WJ, Kim JY, Hao C, Li S, Qu A, Lu M, Wu X, Colombari FM, Gomes WR, Blanco AL, de Moura AF, Guo X, Kuang H, Kotov NA, Xu C. Enantiomer-dependent immunological response to chiral nanoparticles. Nature. 2022;601:366–73.
63. Saito K, Tatsuma T. Chiral plasmonic nanostructures fabricated by circularly polarized light. Nano Lett. 2018;18:3209–12.
64. Morisawa K, Ishida T, Tatsuma T. Photoinduced chirality switching of metal-inorganic plasmonic nanostructures. ACS Nano. 2020;14:3603–9.
65. Kim JY, Yeom J, Zhao GP, Calcaterra H, Munn J, Zhang PJ, Kotov N. Assembly of gold nanoparticles into chiral superstructures driven by circularly polarized light. J Am Chem Soc. 2019;141:11739–44.
66. Chen YP, Xianyu YL, Jiang XY. Surface modification of gold nanoparticles with small molecules for biochemical analysis. Acc Chem Res. 2017;50:310–9.
67. Meng DJ, Chen YD, Ji YL, Shi XH, Wang H, Wu XC. Temperature effect of plasmonic circular dichroism in dynamic oligomers of AuNR@Ag nanorods driven by cysteine: the role of surface atom migration. Adv Opt Mater. 2021;9:2001274.
68. Zhu F, Li XY, Li YC, Yan M, Liu SQ. Enantioselective circular dichroism sensing of cysteine and glutathione with gold nanorods. Anal Chem. 2015;87:357–61.
69. Song M, Tong LM, Liu SL, Zhang YW, Dong JY, Ji YL, Guo Y, Wu XC, Zhang XD, Wang RY. Nonlinear amplification of chirality in self-assembled plasmonic nanostructures. ACS Nano. 2021;15:5715–24.
70. Sun MZ, Xu LG, Fu P, Wu XL, Kuang H, Liu LQ, Xu CL. Scissor-like chiral metamolecules for probing intracellular telomerase activity. Adv Funct Mater. 2016;26:7352–8.
71. Wu XL, Xu LG, Liu LQ, Ma W, Yin HH, Kuang H, Wang LB, Xu CL, Kotov NA. Unexpected chirality of nanoparticle dimers and ultrasensitive chiroplasmonic bioanalysis. J Am Chem Soc. 2013;135:18629–36.
72. Wang ZY, Zhang NN, Li JC, Lu J, Zhao L, Fang XD, Liu K. Serum albumin guided plasmonic nanoassemblies with opposite chiralities. Soft Matter. 2021;17:6298–304.
73. Cheng GQ, Xu D, Lu ZY, Liu K. Chiral self-assembly of nanoparticles induced by polymers synthesized *via* reversible addition-fragmentation chain transfer polymerization. ACS Nano. 2019;13:1479–89.
74. Lu J, Chang YX, Zhang NN, Wei Y, Li AJ, Tai J, Xue Y, Wang ZY, Yang Y, Zhao L, Lu ZY, Liu K. Chiral plasmonic nanochains *via* the self-assembly of gold nanorods and helical glutathione oligomers facilitated by cetyltrimethylammonium bromide micelles. ACS Nano. 2017;11:3463–75.
75. Martens K, Binkowski F, Nguyen L, Hu L, Govorov AO, Burger S, Liedl T. Long- and short-ranged chiral interactions in DNA-assembled plasmonic chains. Nat Commun. 2021;12:2025.
76. Dong JY, Zhou YH, Pan JH, Zhou C, Wang QB. Assembling gold nanobipyramids into chiral plasmonic nanostructures with DNA origami. Chem Commun. 2021;57:6201–4.
77. Martens K, Funck T, Santiago EY, Govorov AO, Burger S, Liedl T. Onset of chirality in plasmonic meta-molecules and dielectric coupling. ACS Nano. 2022;16:16143–9.
78. Pan JH, Wang XY, Zhang JJ, Zhang Q, Wang QB, Zhou C. Chirally assembled plasmonic metamolecules from intrinsically chiral nanoparticles. Nano Res. 2022;15:9447–53.
79. Kumar J, Eraña H, López-Martínez E, Claes N, Martín VF, Solís DM, Bals S, Cortajarena AL, Castilla J, Liz-Marzán LM. Detection of amyloid fibrils in Parkinson's disease using plasmonic chirality. Proc Nat Acad Sci. 2018;115:3225–30.
80. Mokashi-Punekar S, Brooks SC, Hogan CD, Rosi NL. Leveraging peptide sequence modification to promote assembly of chiral helical gold nanoparticle superstructures. Biochemistry. 2021;60:1044–9.
81. Lu XM, Song DP, Ribbe A, Watkins JJ. Chiral arrangements of Au nanoparticles with prescribed handedness templated by helical pores in block copolymer films. Macromolecules. 2017;50:5293–300.
82. Miao T, Cheng X, Ma H, He Z, Zhang PZ, Zhou PN, Zhang PW, Zhu PX. Transfer, amplification, storage, and complete self-recovery of supramolecular chirality in an achiral polymer system. Angew Chem Int Ed. 2021;60:18566–71.
83. Zhang Y, Cui T, Yang J, Huang Y, Ren J, Qu X. Chirality-dependent reprogramming of macrophages by chiral nanozyues. Angew Chem Int Ed. 2023;62: e202307076.
84. Niu X, Zhao R, Yan S, Pang Z, Li H, Yang X, Wang K. Chiral materials: Progress, applications, and prospects. Small. 2023;19:2303059.
85. Rothe M, Zhao Y, Müller J, Kewes G, Koch CT, Lu Y, Benson O. Self-assembly of plasmonic nanoantenna–waveguide structures for subdiffractional chiral sensing. ACS Nano. 2020;15:351–61.
86. Song G, Xu C, Li B. Visual chiral recognition of mandelic acid enantiomers with L-tartaric acid-capped gold nanoparticles as colorimetric probes. Sens Actuators B Chem. 2015;215:504–9.
87. Wang Y, Rao Z, Zhou J, Zheng L, Fu L. A chiral assembly of gold nanoparticle trimer-based biosensors for ultrasensitive detection of the major allergen tropomyosin in shellfish. Biosens Bioelectron. 2019;132:84–9.
88. Horrer A, Zhang Y, Gérard D, Béal J, Kociak M, Plain J, Bachelot R. Local optical chirality induced by near-field mode interference in achiral plasmonic metamolecules. Nano Lett. 2019;20:509–16.
89. Wang G, Zhang H, Kuang H, Xu C, Xu L. Chiral inorganic nanomaterials for bioapplications. Matter. 2023;6:1752–81.
90. Zhou X, Xu C, Jin Y, Li B. Visual chiral recognition of d/l-leucine using cube-shaped gold nanoparticles as colorimetric probes. Spectrochim Acta A. 2019;223: 117263.

91. Hu L, Sun Z, Nie Y, Huang Y, Fang Y. Plasmonic and photonic enhancement of chiral near-fields. Laser Photon Rev. 2022;16:2200035.
92. Wang G, Hao C, Ma W, Qu A, Chen C, Xu J, Xu C, Kuang H, Xu L. Chiral plasmonic triangular nanorings with SERS activity for ultrasensitive detection of amyloid proteins in Alzheimer's disease. Adv Mater. 2021;33:2102337.